

# Emergence of Levy distribution in many-particle quantum systems

A. V. Ponomarev, S. Denisov, and P. Hänggi

*Institute of Physics, University of Augsburg, Universitätsstr. 1, D-86159 Augsburg*

(Dated: March 3, 2019)

Levy distribution, previously used to describe complex behavior of classical systems, are shown to characterize that of quantum many-body systems. Using two complimentary approaches, the canonical and grand-canonical formalisms, we discovered that the momentum profile of  $N$  strongly interacting (hard-core) bosons at finite temperatures on a one-dimensional optical lattice with parabolic confinement obeys Levy distribution. The tunable Levy spline reproduces momentum profiles in the experimentally accessible region up to one recoil momentum. Our finding allows for calibration of complex many-body quantum states by using a unique scaling exponent.

PACS numbers: 05.40.Fb; 67.85.-d; 47.27.eb; 05.30.Jp

## I. INTRODUCTION

Since first observations of quantum collective phenomena, the quantum systems with strongly interacting constituents had become of paramount interest in condense matter community [1]. A new wave of activity in the area of quantum many-body systems has been burgeoning with the advent of laser cooling techniques [2]. Many of those quantum models, which were thought to be theoretical abstractions, has since been implemented with cold atoms [3]. One of such models, a one-dimensional system of hard-core bosons – the Tonks-Girardeau (TG) gas [4] – has been thoroughly probed in recent experiments [5, 6].

While the density profile and the energy spectrum of hard-core bosons resemble that of non-interacting fermions, its momentum distribution (MD) exhibits distinct features. The ground state of a homogeneous TG gas is known to possess an infrared divergence in the thermodynamic limit,  $N \rightarrow \infty$ ,  $n(p) \propto p^{-1/2}$  [7], which, however, vanishes upon addition of a harmonic confinement [8]. So far, there are no analytic results on the infrared behavior of the finite-temperature MD for a finite number bosons in a harmonic trap. In a sole harmonic confinement, the ground-state MD decays as  $n(p) \propto p^{-4}$  in the high momentum regime [9]. Yet in the presence of an optical lattice, which sets an upper momentum scale given by the recoil momentum,  $\hbar k_L$ , where  $k_L$  is the wave vector of the laser beam, this region cannot be resolved with present state-of-the art experiments.

The finite-temperature MDs of  $N \leq 20$  strongly repulsive bosons, confined on a one-dimensional optical lattice and an additional harmonic trap (a so called “1d tube”), have been measured experimentally [5]. These measurements revealed that in the intermediate region,  $0.3 \leq |p/\hbar k_L| \leq 1$ , a momentum profile can be approximated by a power-law,  $n(p) \propto p^{-\gamma}$ . The exponent  $\gamma$  depends on temperature, density, and strength of the atom-atom interactions. Results of numerical Monte-Carlo simulations have corroborated the experimental finding [10].

What kind of momentum distribution emerge in a system of strongly repulsive bosons? In the present work,

we attest that *Levy distribution* describe the MD of  $N$  thermalized hard-core bosons within a single 1d tube as well as within array of 1d tubes probed experimentally [5, 6]. Levy statistics [11] are known to describe classical chaotic transport [12], processes of subrecoil laser cooling [13], fluctuations of stock market indices [14], time series of single molecule blinking events [15], or bursting activity of small neuronal networks [16]. The appearance of Levy distribution in a system output are a strong indicator of a long-range correlation “skeleton” which conducts system intrinsic dynamics [16, 17]. While for non-interacting bosons one expects Bose-Einstein profiles, the Levy distribution have at no time emerged in the context of *many-particle quantum* systems before. The great advantage of the Levy-based analysis is its capability of calibration of the TG in different quantum regimes by a unique scaling exponent  $\alpha$ .

The paper is organized as follows. In Sec. II we introduce the TG model and employ two complimentary approaches to study its finite-temperature properties. In Sec. III we fit exact results of the calculation within the grand-canonical formalism [19] by the Levy distribution. To provide an insight into experimental situation [5], we devoted Sec. IV to the analysis of momentum profiles averaged over the array of 1d tubes. We proceed with the results obtained within the canonical formalism [20] and conclude the section with the analysis of the experimental data from the Ref. [5]. Finally, in Sec. V, we summarize our results. Some of important technical details are deferred to the Appendixes A, B.

## II. TONKS-GIRARDEAU GAS AT FINITE TEMPERATURES

A Bose gas in a deep optical lattice is well described by the Bose-Hubbard Hamiltonian [18]

$$H = -J \sum_l (b_l^\dagger b_{l+1} + h.c.) + \nu \sum_l l^2 n_l + \frac{U}{2} \sum_l n_l (n_l - 1), \quad (1)$$

where  $n_l = b_l^\dagger b_l$  is the particle number operator,  $J$  is the hopping strength, the parabolicity  $\nu = M\omega_0^2 d^2/2$  is the

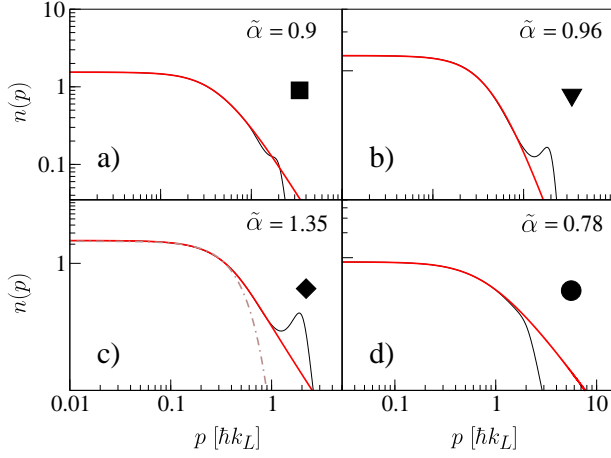


FIG. 1: (color online) Momentum density profiles (MD) for  $N = 40$ (a);  $30$ (b);  $10$ (c);  $90$ (d) hard-core bosons in a 1d tube, thin (black) lines, at four different sets of parameters are compared to Levy distributions, thick (red) line. Dashed-dotted line (c) corresponds to a Gaussian approximation. The parameters  $(N/n_s, k_B T/J)$  are indicated by symbols  $\blacklozenge$ ,  $\blacktriangledown$ ,  $\blacksquare$ ,  $\bullet$  in Fig. 2.

amplitude of the external parabolic potential with the trapping frequency  $\omega_0$ ,  $M$  is the mass of the atom, and  $d$  is the lattice constant. The last term in (1) describes the on-site atom-atom interactions. Here we are interested in the TG regime, where the strength of the repulsive atom-atom interaction considerably exceeds the kinetic (hopping) energy, i.e.,  $U/J \rightarrow \infty$ , [4]. Therefore, the interaction term can be substituted by the condition that two bosons cannot occupy the same lattice site [4].

The momentum distribution can be obtained from the reduced single-particle density matrix  $\rho_{n,l}$ , reading

$$n(p) = |\Phi(p)|^2 \sum_{n,l} e^{-ip(n-l)} \rho_{n,l}, \quad (2)$$

where the momentum  $p$  is written in units of recoil momentum  $\hbar k_L = \pi \hbar/d$ , and the envelope  $\Phi(p)$  is the Fourier transform of the Wannier function. Note that the latter, as well as the hopping  $J$ , is solely defined by the lattice depth,  $V_0$ , measured in units of recoil energy,  $E_R = (\hbar k_L)^2/2M$ .

To find the reduced single-particle density matrix, we employ here the grand-canonical [19] and the canonical formalism [20] (See Appendixes A, B). The first is relevant for a system being in contact with a thermal cloud at constant temperature  $T$ , while the second describes an isolated many-particle system.

The difference between the momentum distributions obtained within the grand-canonical and the canonical descriptions is mediated by the number of particles and becomes negligible for  $N \gtrsim 10$  [19]. In addition, at finite temperatures  $k_B T \gtrsim 0.1J$ , systems with different number of particles, but the same densities  $N/n_s$ , possess the same momentum profiles [19]. Here,  $n_s = 8(J\nu)^{1/2}/\pi$  is

the number of single-particle eigenstates with non-zero population at the trap center [21]. The latter also yields the critical number of bosons in a 1d tube required to form the Mott-insulator in the trap center at zero temperature.

The typical examples of the MD obtained here within the grand-canonical formalism are presented in Fig. 1 for  $N \geq 10$ , where the results of both the grand-canonical and canonical descriptions practically identical.

### III. LEVY SPLINE APPROXIMATION

In view of the strong non-Gaussian behavior of the function  $n(p)$  (see Fig. 1c) and an apparent power-law intermediate asymptotics [5, 10], it is tempting to compare the MD of the TG gas with symmetric Levy distribution [11]. The latter,  $L_\alpha(p)$ , is a natural generalization of the Gaussian distribution, and it is defined by the Fourier transform of its characteristic function; i.e.,

$$L_\alpha(p) = \frac{1}{2\pi} \int_{-\infty}^{\infty} \varphi(\xi) e^{ip\xi} d\xi, \quad \varphi(\xi) = \exp(-C_\alpha |\xi|^\alpha), \quad (3)$$

where the exponent  $0 < \alpha \leq 2$ , and  $C_\alpha > 0$  is some constant [11]. For  $\alpha = 2$  the distribution is Gaussian. The value of  $\alpha$  is invariant under the scaling transformation  $p \rightarrow \text{const} \cdot p$ , which can be used for fitting.

The Levy distribution exhibits a power-law asymptotics,  $L_\alpha(p) \propto p^{-(\alpha+1)}$ , as  $|p| \rightarrow \infty$ . These “heavy” tails cause the variance of Levy distributions to diverge for all  $\alpha < 2$ . However, this asymptotic limit is not relevant for our objective: the MD for the system (1) is bounded by the width of  $|\Phi(p)|$ ,  $(V_0/E_R)^{1/4} \hbar k_L$  [10], so that the MD variance remains finite.

The fitting of the calculated MD  $n(p)$  by the Levy distribution  $L_\alpha(p)$  was automatized and performed numerically by the global minimum search of the mean square deviation,  $\Delta = \sum_n \{[n(p_n) - L_\alpha(p_n)]^2/n(0)\}^{1/2}$ , in a 2d parametric space  $\{\alpha, C_\alpha\}$  (3). For the results shown on Figs. 1,2, we took 50 spline points equally spaced on the interval  $p \in (0, \hbar k_L)$ . The initial area,  $\alpha \in (0, 2)$ ,  $C_\alpha \in (0, 30)$ , covered by  $10 \times 10$  grid was iteratively converged to the global minimum by decreasing the grid step in  $\alpha$  and  $C_\alpha$  until the desired relative accuracy (fixed to 1% in all figures) was reached.

In Fig. 2, we show the dependence of scaling exponent  $\alpha$  (top) on the scaled temperature  $k_B T/J$  and scaled particle density,  $N/n_s$  (obtained for  $N = 10, \dots, 100$ , and  $n_s = 48.78$ ), together with the associated mean square deviation  $\Delta$  (bottom), at relatively low and high amplitude of the optical lattice. These diagrams (see also Fig. 1, for concrete examples of MD and their Levy-spline approximations) constitute a first main result of this work, namely, the convergence of MD of TG gas towards the Levy distribution with increasing temperature.

Despite of infinitely strong on-site repulsive interactions, the systematic increase of the Levy exponent  $\alpha$

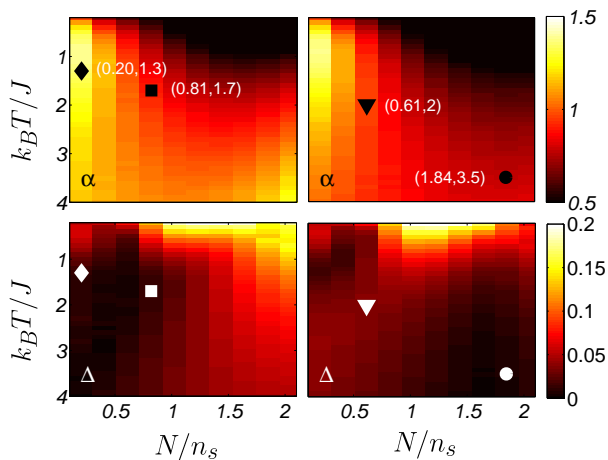


FIG. 2: (color online) The scaling exponent of Levy distribution,  $\alpha$  (top), and corresponding mean square deviation from the exact momentum density profile,  $\Delta$  (bottom), of TG gas as a function of temperature and particle density for two different amplitudes of the optical lattice,  $V_0 = 4.6E_R$  (left column), and  $V_0 = 9.3E_R$  (right column), see text for more details. The amplitude of parabolic confinement is chosen as  $\nu = 2 \cdot 10^{-4} E_R$ .

with temperature, cf. Fig. 2 (top), is consistent with the high-temperature limit where the ideal Bose gas obeys the classical Boltzmann-Maxwell statistics with a Gaussian MD, i.e.,  $\alpha = 2$ .

#### IV. AVERAGING OVER THE ARRAY OF 1D TUBES

The single 1d tube realization, using a fixed temperature  $T$  and fixed particle number  $N$ , is not directly accessible with the present state-of-art experiments. The averaging over an array of tubes done in Ref. [5] can be understood as an averaging over many realizations, with different parameters,  $T$  and  $N$ .

Namely, the experimental setup [5] produces an array of independent 1d tubes, with different numbers,  $N_i$ , of particles. The probability of having a tube with  $N$  particles is given by [5]

$$\varrho(N) = \frac{2}{3} \frac{1}{N_c^{2/3} N^{1/3}}, \quad N \leq N_c, \quad (4)$$

where  $N_c$ , i.e. the number of particles in a central tube, is a unique parameter. Assuming the same initial temperature in all the tubes for the shallow 1d lattice potential,  $V_{in}$ , the temperatures at the experimentally adjusted lattice depth,  $V_0$ , can be obtained by using the conservation of entropy in each tube during the subsequent adiabatic increase of the lattice depth from  $V_{in}$  to  $V_0$ . Therefore, tubes with different number of particles,  $N_i$ , acquire different final temperatures,  $T_i$ , at  $V_0 > V_{in}$  [5].

We implemented this averaging procedure with  $N_c = 18$ , for a set of individual MDs pre-calculated within the

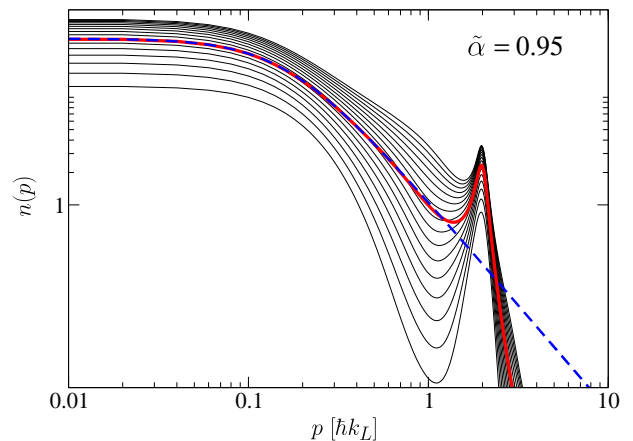


FIG. 3: (color online) Momentum distributions (MD) for  $N = 3, \dots, 18$  hard-core bosons, thin (black) lines, obtained within the canonical approach (B1) and the MD averaged over the array of 1d tubes according to the experimental procedure used in Ref. [5], thick (red) line, with its best Levy-spline, thick (blue) dashed line.

canonical formalism. The result for  $k_B T = 0.5J$ ,  $V_0 = V_{ini} = 4.6E_R$  and  $\nu = 8 \cdot 10^{-4} E_R$  is depicted in Fig. 3.

Surprisingly enough, the averaged MD can be perfectly approximated by the Levy distribution with an “average” scaling exponent,  $\tilde{\alpha}$ ; this is so despite the sizable dispersion of  $\alpha$ -values appearing in the different momentum profiles.

Therefore, the averaged momentum profile appears as a superposition of several different profiles. It is known that using a proper weight function,  $f(\beta)$ , one can construct a Levy distribution from a parameterized set of Gaussian distributions of different dispersion,  $L_\alpha(p) = \int_{-\infty}^{\infty} G(p, \beta) f(\beta) d\beta$  [23]. Yet, to the best of our knowledge, there are no results concerning the superposition of many different Levy functions of *different exponents*  $\alpha$ .

A next objective is the comparison of our scheme with the experimental data from Ref.[5], see Fig.4. As one can deduce the Levy distribution yields an excellent approximation for the MD of the experimental system although the latter does not map precisely to the TG gas, but rather corresponds to a set of  $N$  soft-core bosons with  $U/J < \infty$  (1) [10]. In the experiment, one used an intermediate range only ( $0.3 \leq |p/\hbar k_L| \leq 1$ ) power-law fit,  $n(p) \propto p^{-\gamma_{exp}}$  [5], with  $\gamma_{exp} - 1 = 1.2; 0.9; 0.4; 0.2$  for the data shown on Figs. 4(a-d), respectively. We emphasize, however, that in the experimentally accessible region,  $|p| \lesssim 2\hbar k_L$ , the power law behavior with the exponent  $\gamma_{exp} - 1 = \tilde{\alpha}$  of the Levy distribution are not yet valid, but is assumed only for much larger momentum values. Therefore, the theoretical estimates  $\tilde{\alpha}$  in Fig. 4 exceed those intermediate, experimentally fit-values, i.e. one consistently finds that  $\tilde{\alpha} > \gamma_{exp} - 1$ .

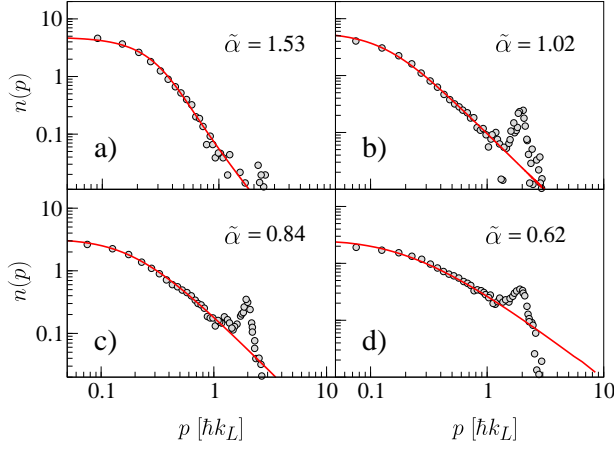


FIG. 4: (color online) The experimental data for the MD of the 1d quantum gases for different axial lattice depths [5], grey dots; Levy distributions with the scaling exponent  $\tilde{\alpha}$ , solid (red) lines.

## V. CONCLUSIONS

We have presented a study of finite-temperature momentum profiles of Tonks-Girardeau gases confined on 1d lattices. The momentum distribution (MD) depends on the number of bosons, the lattice depth and the gas temperature. We have shown that the tunable Levy distribution fits momentum profiles up to one recoil momentum with high accuracy. This allows for calibration of TG states with a unique scaling exponent. Thus, our approach completes the attempts to quantify the finite-temperature MDs by using a power-law fitting for the intermediate region  $0.3 \leq |p/\hbar k_L| \leq 1$  [5, 10].

We want to stress one aspect which we consider as crucial for the understanding of our approach. It is well known that the Levy distribution has appeared as the stable distribution, i.e. the “attractor” for normalized sums of independent and identically-distributed random variables, with no finite mean values. The latter has opened the door to anomalous *statistics* [11]. In our approach, we employ the Levy distribution (3) merely as the *mathematical function*, which is a natural generalization of the standard Gaussian function, thus leaving aside all the possible statistical interpretations and speculations concerning physical processes responsible for the MD formation. A good example for such “applied” approaches we mention is the use of the Gaussian distribution, which describes the wave function of the ground state of the quantum harmonic oscillator [24], the Green’s function solution of the deterministic heat or diffusion equation [25], and frequently results as a form function in many different physical contexts.

The Levy distribution is not a peculiarity of confined TG gases only. Preliminary numerical analysis demonstrates that the MD of  $N$  strongly interacting fermionic atoms in a sole harmonic confinement [26] also obeys the Levy distribution function (3). We thus con-

jecture that Levy distribution functions may results as a generic feature of quantum many-particle systems with strong interparticle interactions.

While it is intuitively clear that it is the long-range correlations in the system that cause the emergence of Levy distributions, the task to unravel the inherent physical mechanism(s) yielding this anomalous distribution remains a challenge. We think that the analysis of a reduced single-particle density matrix in a spirit of the theory of random Levy matrices [28] may shed additional light on this intriguing issue.

## Acknowledgments

This work was supported by the DFG through grant HA1517/31-1 and by the German Excellence Initiative “Nanosystems Initiative Munich (NIM)”.

## APPENDIX A: GRAND-CANONICAL FORMALISM

Within the grand-canonical description, the number of bosons,  $N$ , is a fluctuating quantity and the reduced single-particle density matrix is defined as the trace over the Fock space,

$$\rho_{n,l} = \frac{1}{Z} \text{Tr} \left\{ \langle b_n^\dagger b_l \rangle e^{-\beta(H - \mu \sum_j n_j)} \right\}, \quad (\text{A1})$$

where the chemical potential  $\mu$  is fixed to give the required number of particles  $N = \sum_l \rho_{l,l}$  in the system,  $\beta = 1/k_B T$  with  $k_B$  being the Boltzmann factor, and  $Z$  is the grand-canonical partition function. The latter coincides with that of non-interacting fermions, i.e.,  $Z = \prod_j [1 + e^{-\beta(\epsilon_j - \mu)}]$ , where  $\epsilon_j$  stands for the single-particle energy spectrum.

The trace over the the Fock space (A1) can be evaluated exactly [19] by mapping the problem of hard-core bosons on that of spinless fermions via the Jordan-Wigner transformation [29]. We next use the expressions for the elements of the reduced single-particle density matrix elaborated in [19], i.e.,

$$\rho_{n,l} = \frac{1}{Z} \left\{ \det [\mathbf{I} + (\mathbf{I} + \mathbf{A}(n,l))\mathbf{D}(n,l)] - \det [\mathbf{I} + \mathbf{D}(n,l)] \right\}, \text{ for } n \neq l, \quad (\text{A2})$$

$$\mathbf{D}(n,l) = \mathbf{O}(l) \mathbf{U} e^{-(\mathbf{E} - \mu \mathbf{I})/k_B T} \mathbf{U}^\dagger \mathbf{O}(n); \quad (\text{A3})$$

and

$$\rho_{n,n} = \left[ \mathbf{U} \left( \mathbf{I} + e^{(\mathbf{E} - \mu \mathbf{I})/k_B T} \right)^{-1} \mathbf{U}^\dagger \right]_{n,n}, \quad (\text{A4})$$

for the main diagonal elements. All operators entering above are the square matrices  $N \times N$  defined as follows:  $\mathbf{I}$  denotes the identity matrix,  $\mathbf{O}(n)_{i,j} = \{-\delta_{i,j}, i \leq$

$n-1; \delta_{i,j}, i > n-1\}$ ,  $\mathbf{A}(n, l)_{i,j} = \delta_{i,n} \delta_{j,l}$ ,  $\mathbf{U}$  is the orthogonal matrix of eigenvectors satisfying the eigenproblem,  $H_1 \mathbf{U} = \mathbf{U} \mathbf{E}$ , with single-particle version of Hamiltonian (1)

$$H_1 = -J \sum_l (|l+1\rangle \langle l| + h.c.) + \nu \sum_l l^2 |l\rangle \langle l|, \quad (\text{A5})$$

and  $\mathbf{E}$  is diagonal matrix of its eigenvalues, i.e.,  $\mathbf{E}_{i,j} = \varepsilon_i \delta_{i,j}$ . Thus, to obtain the entire matrix  $\rho_{n,l}$  ( $\rho_{l,n} = \rho_{n,l}^*$ ) one has to compute  $N(N-1)/2$  determinants of  $N \times N$  matrices.

## APPENDIX B: CANONICAL FORMALISM

In the canonical formalism, the particle reservoir is absent, meaning that one has to find the number,  $\mathcal{N}_e$ , self-consistently from those many particle states,  $|\Psi^n\rangle$ , together with their eigenenergies,  $E_n$ , that contribute to the thermal superposition at a given temperature. The reduced single-particle density matrix is then obtained as a sum of thermally weighted density matrices evaluated for each eigenstates separately; i.e.,

$$\rho_{n,l} = \frac{1}{\mathcal{Z}} \sum_{m=1}^{\mathcal{N}_e} e^{-\beta E_m} \rho_{n,l}^m, \quad (\text{B1})$$

where  $\rho_{n,l}^m = \langle \Psi^m | b_n^\dagger b_l | \Psi^m \rangle$ . The canonical partition function  $\mathcal{Z}$  is expressed through the true many particle energy spectrum:  $\mathcal{Z} = \sum_{m=1}^{\mathcal{N}_e} e^{-\beta E_m}$ .

The energy spectrum of hard-core bosons is the same as that for spinless fermions:  $E_m = \sum_{n=1}^N \epsilon_{\alpha_n^m}$ , where

$\alpha_n^m$  denotes the numbers of single-particle eigenlevels occupied in the  $m$ -th many-particle state.

The corresponding many-particle eigenstates can be represented as

$$|\Psi^m\rangle = \prod_{\alpha_n^m} \sum_l \mathbf{U}_{l, \alpha_n^m} b_l^\dagger |0\rangle, \quad n = 1, \dots, N \quad (\text{B2})$$

where  $\mathbf{U}$  is complete orthogonal set of single-particle eigenvectors (see Appendix A).

Each contribution,  $\rho_{i,j}^m$ , is related to the Green function,  $G_{i,j}^m = \langle \Psi^m | b_i b_j^\dagger | \Psi^m \rangle$ :

$$\rho_{i,j}^m = G_{i,j}^m + \delta_{i,j} (1 - 2G_{i,j}^m). \quad (\text{B3})$$

Using the Jordan-Wigner transformation [29], the bosonic Green function can be rewritten as scalar product of two fermionic wave-functions, and subsequently as a determinant of matrix product [20]:

$$G_{i,j}^m = \det [(\mathbf{P}^m(i))^\dagger \mathbf{P}^m(j)], \quad (\text{B4})$$

where the matrix  $\mathbf{P}^m(k)_{l,n}$  has  $N+1$  columns

$$\mathbf{P}^m(k)_{l,n} = \begin{cases} -\mathbf{U}_{l, \alpha_n^m}, & \text{for } l \leq k-1, n = 1, \dots, N; \\ \mathbf{U}_{l, \alpha_n^m}, & \text{for } l > k-1, n = 1, \dots, N; \\ \delta_{k,l}, & \text{for } n = N+1. \end{cases} \quad (\text{B5})$$

In comparison to the grand-canonical approach, the number of operations needed to obtain the entire matrix  $\rho_{i,j}$  is a factor of  $\mathcal{N}_e$  larger, and is growing with increasing temperature.

- 
- [1] D. J. Thouless, *The Quantum Mechanics of Many-body Systems* (Academic Press, New York, 1972); A. L. Fetter and J. D. Walecka, *Quantum Theory of Many-Particle Systems* (Dover, New York, 2003).
  - [2] H. J. Metcalf and P. van der Straten, *Laser Cooling and Trapping* (Springer, New York, 1999).
  - [3] O. Morsch and M. Oberthaler, Rev. Mod. Phys. **78**, 179 (2006).
  - [4] M. Girardeau, J. Math. Phys. **1**, 516 (1960).
  - [5] B. Paredes *et al.*, Nature **429**, 277 (2004).
  - [6] T. Kinoshita, T. Wenger, and D. S. Weiss, Science **305**, 1125 (2004).
  - [7] M. Olshanii and V. Dunjko, Phys. Rev. Lett. **91**, 090401 (2003).
  - [8] T. Papenbrock, Phys. Rev. A **67**, 041601(R) (2003).
  - [9] A. Minguzzi, P. Vignolo, and M. P. Tosi, Phys. Lett. A **294**, 222 (2002).
  - [10] L. Pollet, S. M. A. Rombouts, and P. J. H. Denteneer, Phys. Rev. Lett. **93**, 210401 (2004).
  - [11] W. Feller, *An Introduction to Probability Theory and Its Applications* (John Wiley and Sons, New York, 1970), Vol.2.
  - [12] M. F. Shlesinger, G. M. Zaslavsky, and J. Klafter, Nature **363**, 31 (1993); A. Blumen, G. Zumofen, and J. Klafter, Phys. Rev. A **40**, 3964 (1989).
  - [13] F. Bardou, J.-P. Bouchaud, A. Aspect and C. Cohen-Tannoudji, *Levy Statistics and Laser Cooling* (Cambridge Univ. Press, Cambridge 2000).
  - [14] R. N. Mantegna and H. E. Stanley, Nature **376**, 46 (1995).
  - [15] E. Barkai, R. Silbey, and G. Zumofen, Phys. Rev. Lett. **84**, 5339 (2000).
  - [16] R. Segev *et al.*, Phys. Rev. Lett. **88**, 118102 (2002).
  - [17] C.-K. Peng *et al.*, Phys. Rev. Lett. **70**, 1343 (1993).
  - [18] D. Jaksch, C. Bruder, J. I. Cirac, C. W. Gardiner, and P. Zoller, Phys. Rev. Lett. **81**, 3108 (1998).
  - [19] M. Rigol, Phys. Rev. A **72**, 063607 (2005).
  - [20] M. Rigol and A. Muramatsu, Phys. Rev. A **70**, 031603(R) (2004); *ibid.*, **72**, 013604 (2005).
  - [21] The critical density  $n_s$  is found via mapping the single particle version of (1) onto the quantum pendulum [22].
  - [22] A. V. Ponomarev and A. R. Kolovsky, Laser Phys. **16**, 367 (2006).
  - [23] C. Beck and E. G. D. Cohen, Physica A **322**, 267 (2003).
  - [24] R. L. Liboff, *Introductory Quantum Mechanics* (Addison-Wesley, London, 2002).

- [25] G. Barton, *Elements of Green's functions and Propagation* (Clarendon press, Oxford, 1989).
- [26] A. V. Ponomarev, S. Denisov and P. Hänggi, *unpublished*.
- [27] I. Bloch, J. Dalibard, and W. Zwerger, Rev. Mod. Phys. **80**, 885 (2008).
- [28] P. Cizeau and J. P. Bouchaud, Phys. Rev. E **50**, 1810 (1994).
- [29] P. Jordan and E. Wigner, Z. Phys. **47**, 631 (1928).